Applied Catalysis B: Environmental 181 (2016) 249–259

Contents lists available at ScienceDirect

Applied Catalysis B: Environmental

journal homepage: www.elsevier.com/locate/apcatb

On the optimization of activated carbon-supported iron catalysts in catalytic wet peroxide oxidation process

A. Rey[a], A.B. Hungria[b], C.J. Duran-Valle[c], M. Faraldos[a], A. Bahamonde[a,a,*], J.A. Casas[d], J.J. Rodriguez[d]

[a] Instituto de Catálisis y Petroleoquímica, CSIC, C/ Marie Curie 2, 28049 Madrid, Spain
[b] Dept Ciencia de los Materiales e Ingeniería Metalúrgica y Química Inorgánica, Universidad de Cádiz, 11510 Cádiz Spain
[c] Departamento de Química Orgánica e Inorgánica and ACYS, Universidad de Extremadura, Avd. Elvas S/N, 06006 Badajoz, Spain
[d] Sección de Ingeniería Química, Facultad de Ciencias, Universidad Autónoma de Madrid, C/ Francisco Tomás y Valiente 7, 28049 Madrid, Spain

ARTICLE INFO

Article history:
Received 30 March 2015
Received in revised form 21 July 2015
Accepted 25 July 2015
Available online 1 August 2015

Keywords:
Iron particles
Activated carbon
CWPO
Hydrogen peroxide
Hydroxyl radicals

ABSTRACT

Different homemade iron-activated carbon catalysts (Fe/AC) have been studied in the CWPO of phenol at mild conditions (atmospheric pressure and 50 °C). Both iron content and the way to introduce iron active phase in Fe/AC catalysts were analyzed to select the most stable and efficient activated carbon-supported iron catalyst. The major differences were found on their surface properties, mainly those related to iron distribution and iron particle size. Catalysts prepared by two-consecutive steps of impregnation, regardless of iron content, always presented lower leaching phenomena of iron to the reaction medium than those prepared by one-step wetness impregnation. This higher stability could be indicating an improved metal-support interaction as a consequence of the two-step methodology used to incorporate the iron, which leads to the formation of small iron particles very homogeneous in size (≈3 nm). The best performance balanced between activity and stability was obtained with 2% iron 2-steps catalyst (2sFe/CN) which gave rise to complete removal of phenol after 60 min, maximal reduction of TOC content and optimal use of the stoichiometric amount of H_2O_2 added during batch experiments at 50 °C, atmospheric pressure, 500 mg L^{-1} catalyst loading, 100 mg L^{-1} and 500 mg L^{-1} of phenol and hydrogen peroxide concentrations, respectively, at $pH_0 = 3$.

The study of H_2O_2 decomposition in the presence of an excess of MeOH, a well-known •OH scavenger, has been an useful tool to analyze the behavior of heterogeneous catalysts in CWPO reactions. 2sFe/CN catalyst led to a better and efficient use of H_2O_2 with higher hydroxyl radical yield in the presence of phenol instead of methanol, as a consequence of phenol adsorption onto the catalyst surface which minimizes the inefficient decomposition of H_2O_2 at the same operating conditions.

1. Introduction

During the past few decades, people, governments and scientific community have recognized the potential for recovering water from wastewaters emerging as a vital component of sustainable water resources management in the 21st century [1], adopting in this line, the European Directive 2000/60/CE [2], forces the need to adopt measures against water pollution to search novel methods in the near future [1].

The production of wastewaters, from both industrial and domestic uses generates a variety of effluents requiring specific treatments. To manage these wastes a number of different techniques such as chemical, physical, biological, incineration, etc. [3], and their combinations are available, but each process has its intrinsic limitations in applicability, effectiveness, and cost [4]. Many industrial waste streams are not suitable for biological processes due to inherent toxicity and the presence of some pollutants highly refractory, besides their treatment by traditional non-catalytic chemical processes or by incineration may be too energy consuming [5]. Therefore more efficient and economic solutions for end-stream treatment, avoiding higher-energy input technologies are becoming imperative [6] and essential to produce reusable processed water and environmentally friendly effluents.

Among alternative treatment technologies [7,8], advanced oxidation processes (AOPs) that usually operate at or near ambient temperature and pressure [9], have the possibility of exploiting

* Corresponding author. Fax: +34 915854760.
E-mail address: abahamonde@icp.csic.es (A. Bahamonde).

http://dx.doi.org/10.1016/j.apcatb.2015.07.051
0926-3373/

the high reactivity of OH in driving oxidation processes. AOPs options based on heterogeneous catalysts are adequate techniques for wastewater treatments with low to moderate organic contents [10].

Although different iron supported activated-carbon catalysts with very high activity towards oxidation of organic pollutants have been successfully synthesized and tested in the oxidation of phenol [11,12], no important advances about the knowledge of the efficiency of hydroxyl radical production in the catalytic phenol oxidation have been still addressed. It is known that hydrogen peroxide decomposition can be activated on AC surfaces involving the formation of inactive O_2 with or without •OH free radicals as intermediate species [13–15]. At the same time iron species on the Fe/AC catalyst surface are also able to form hydroxyl radicals during phenol oxidation [11]. Hence, it would be desirable to know the H_2O_2 selectivity towards •OH formation to try to elucidate the efficiency of hydroxyl radical production during hydrogen peroxide decomposition in CWPO of phenol with iron activated carbon based catalysts (Fe/AC).

Therefore, the aim of this work has been double: firstly, choose an optimal iron-activated carbon based catalyst that acts efficiently in the phenol degradation by promoting H_2O_2 decomposition to •OH radicals, and producing the lowest amount of inactive molecular oxygen. For that, all the Fe/AC catalysts prepared were tested in H_2O_2 decomposition in the presence and absence of methanol, a known strong scavenger of hydroxyl radicals, to investigate the selectivity towards •OH formation in this reaction and their behavior in the CWPO of phenol. Secondly, minimize the concentration of iron release to the solution during phenol oxidation reaction to avoid any additional pollution and the catalyst deactivation. For this purpose, both iron content and the way to introduce iron active phase in Fe/AC catalysts were investigated in the CWPO of phenol, to select the most stable and efficient activated carbon-supported iron catalyst.

2. Experimental

2.1. Catalysts preparation

Different carbon-supported iron catalysts were obtained with a commercial activated carbon material (CN) supplied by Norit (Norit Row 0.8 Supra; $d_p < 0.6$ mm) whose characteristics are described elsewhere [14]. Three of the studied catalysts (1Fe/CN, 2Fe/CN and 4Fe/CN) were prepared by incipient wetness impregnation of the commercial activated carbon (CN) with an aqueous solution of iron(III) nitrate nonahydrate ($Fe(NO_3)_3 \cdot 9H_2O$) (Merck), with 1, 2, and 4 wt.% of iron nominal content, respectively. Then, all the catalysts were dried at room temperature for 4 h, subsequently at 60 °C for 12 h and finally heat-treated at 250 °C for 4 h in air atmosphere.

The other two iron supported catalysts (4sFe/CN and 2sFe/CN) were prepared by a modified incipient wetness impregnation method, where the iron nitrate was incorporated in two steps, with the same heat-treatment described above after each step, to finally introduce 4 and 2 wt. % of iron nominal content, respectively. Lastly, another iron supported catalyst (4Fe/CNO) was obtained by modification of the original activated carbon support for comparative purpose. This CNO support was the result of treating the original commercial activated carbon with HNO_3 solution (65%) at room temperature for 4 h (1 g AC/12.5 mL HNO_3 solution). Following, the sample was washed with distilled water and dried overnight at 80 °C, subsequently a heat-treatment at 200 °C for 4 h in air atmosphere was applied. All the catalysts were milled and sieved to obtain particles size in the range 63–100 μm. Table 1 summarizes the identification of the prepared catalysts.

Table 1
Catalysts identification and synthesis procedure.

Catalyst	Support	Fe (%)	Impregnation procedure
1Fe/CN	CN	1	1 step
4Fe/CN	CN	4	1 step
4Fe/CNO	CNO	4	1 step
2Fe/CN	CN	2	1 step
4sFe/CN	CN 2Fe/CN	4	2 steps
2sFe/CN	CN 1Fe/CN	2	2 steps

2.2. Catalysts characterization

Elemental analyses were performed by an Elemental Analyzer LECO CHNS-932. Iron content determination of previously digested Fe/AC catalysts was carried out by inductively coupled plasma technique (ICP-OES) with a Perkin Elmer Model Optima 3300DV.

Thermal gravimetry and differential temperature analyses (TG-DTA) were performed with a Mettler Toledo TGA/STD A 851e using the following conditions: air flow of 250 $cm^3\ min^{-1}$ at a heating rate of 10 °C min^{-1} from room temperature to 1000 °C.

Specific surface areas, S_{BET}, were obtained from nitrogen adsorption data, at −196 °C using a Micromeritics Tristar apparatus, after application of the BET equation [16] in the range of 0.02–0.15 relative pressures, for microporous samples. Prior to N_2 adsorption the samples were outgassed overnight at 250 °C, at a pressure $<10^{-4}$ Pa to ensure a dry clean surface, free from any loosely held adsorbed species. Micro and mesopore volumes and the external or non-microporous surface were estimated by means of the *t*-method. Meso and macropore volumes determination was completed by mercury intrusion porosimetry (MIP) using a CE Instrument Pascal 140/240 and applying the Washburn equation, with the values recommended by the IUPAC of 141° and 484 mN m^{-1}, for the contact angle and surface tension of mercury, respectively.

Determination of aqueous slurries pH of catalysts was carried out by placing 0.5 g of the catalyst and 10 mL of CO_2-free distilled water in a bottle, kept continuously stirred at room temperature until pH of the slurry was invariable. pH measurements were performed after filtration in a Crison pH-meter.

The nature, distribution and amount of surface oxygen groups of activated carbon supports and Fe/AC catalysts were analyzed by temperature programmed desorption under N_2 flow (TPD-N_2) and by X-ray photoelectron spectroscopy (XPS). This second technique was also used to identify Fe species. For TPD analyses a sample amount of 0.1 g was placed in a vertical quartz tube in nitrogen flow of 1 NL min^{-1} at a heating rate of 10 °C min^{-1} from room temperature to 900 °C. The evolved amount of CO and CO_2 was continuously registered by a Siemens Ultramat 23 NDIR analyzer.

X-ray photoelectron spectra (XPS) were recorded with a VG Escalab 200R spectrometer equipped with a hemispherical electron analyzer (pass energy of 20 eV) and a Mg Kα ($h\nu = 1254.6$ eV) X-ray source, powered at 120 W. Binding energies were calibrated relative to the C 1s peak of carbon samples at 284.6 eV. For the analysis of the peaks a Shirley type background was used. Peaks were adjusted to a combination of Gaussian and Lorentzian functions using the XPSPeak 4.1 software.

The metal dispersion and nature of the catalysts was investigated using high angle annular dark field scanning transmission electron microscopy (HAADF-STEM) images acquired in a JEOL 2010 F transmission electron microscope (TEM), equipped with an EDS spectrometer Oxford INCA Energy 2000 system. The distribution and size of iron particles were calculated counting for each catalyst around 1000 particles from 10 different micrographs.

2.3. CWPO of phenol

Catalytic wet peroxide oxidation runs were carried out in a 50 mL batch reactor at 50 °C, pH 3, atmospheric pressure, and the following starting concentrations: 100 mg L^{-1} of phenol and 500 mg L^{-1} of H_2O_2 that corresponds to the stoichiometric amount for complete oxidation of phenol. Powdered iron-activated carbon catalyst ($d_{particle}$ between 63 and 100 μm) was added into the reactor at a concentration of 500 mg L^{-1}. Phenol adsorption runs were performed at the same operating conditions without H_2O_2 addition.

A long-term stability test (180 h) was carried out in continuous operation mode in a 250 mL glass-made stirred tank reactor (CSTR) supplied with magnetic stirring (650 rpm). An aqueous solution of phenol (100 mg L^{-1}) and H_2O_2 (500 mg L^{-1}) at acidic pH 3 was continuously fed to the reactor using a peristaltic pump at 1 mL min^{-1} flow rate. The catalyst loading was 0.5 g which means a space time value (W/Q_L) of 500 g min L^{-1}. The reaction volume was maintained with a second channel of the peristaltic pump using a filter of 0.2 μm to avoid the loss of catalyst (powdered catalyst had particle sizes between 63 and 100 μm). Temperature was kept at 50 °C throughout the experiment.

Phenol and aromatic intermediate compounds as well as short-chain organic acids were followed by HPLC (Varian 920LC) with photo-diode array detector. A Polaris C18A 3 μm column (25 cm long, 4.6 mm diameter) was used as stationary phase at 30 °C. Mobile phase flow was 1 mL min^{-1} and methanol/acidic water (0.1% phosphoric acid) were used as eluents, with a linear gradient 0–20% MeOH after short-chain organic acids elution. Total organic carbon (TOC) was measured with a TOC-VSHs Analyzer (Shimadzu). Hydrogen peroxide concentration was determined by a colorimetric titration method [17] based on the formation of a yellow colored Ti(IV)-H_2O_2 complex, using a UV 2100 Shimadzu UV/Vis spectrophotometer at 410 nm. The concentration of iron lixiviates from catalysts to the reaction media was quantified by the o-phenantroline method [18], using an UV/Vis spectrophotometer at 510 nm.

The organic matter adsorbed onto Fe/AC catalyst was extracted by mixing 20 mg of the used catalyst with 50 mL of 1 M NaOH solution (pH=12) at 85° C under continuous stirring during 5 hours. At these conditions of pH and temperature, phenol and its main oxidation by-products desorption take place by the formation of their corresponding sodium salts [16–18]. After the NaOH treatment, the catalyst was filtered and the TOC of the filtrate was measured. Previous experiments with known amounts of phenol, catechol, hydroquinone and p-benzoquinone absorbed onto Fe/AC catalysts led to 90% TOC recovery.

2.4. Hydrogen Peroxide decomposition

Two types of experiments were carried out to analyze hydrogen peroxide decomposition reaction. First, to follow H_2O_2 evolution along reaction time, runs in batch reactors using 100 mL glass bottles shaken in a thermostatic batch were carried out with and without methanol, at the following operating conditions: 200 rpm, 50 °C, atmospheric pressure, 50 mL of reaction volume and initial pH=3 adjusted by using concentrated HCl solution. Initial concentrations were the following: 500 mg L^{-1} of H_2O_2, 500 mg L^{-1} of powered catalyst (d_p < 100 μm) loading, and 20 g L^{-1} of MeOH, only in the case of quenching runs. Hydrogen peroxide concentration was determined as reported above. The other type of H_2O_2 decomposition runs were carried out in a discontinuous batch reactor, with and without methanol, following only the oxygen formation along reaction time. The operating conditions were the following: $V_{reactor}$ = 500 mL, 700 rpm, atmospheric pressure, 50 °C, pH_0 3, 500 mg L^{-1} of H_2O_2, 500 mg L^{-1} of powered catalyst (d_p < 100 μm) loading and 20 g L^{-1} of MeOH. The initial concentration of methanol in both types of experiments was selected taking into account a previous study [19].

Measurement of the O_2 (g) evolved upon H_2O_2 decomposition at atmospheric pressure and 50 °C was carried out by a graduated cylinder which was immersed in a water bath at room temperature, and linked to the reactor through a flexible hose, provided with a CO_2 trap. Oxygen volume was corrected every time taking into account the corresponding pressure value of the water column. A previous study in homogeneous conditions with 20 and 100 mg L^{-1} of Fe^{2+} confirmed that the used concentration of methanol was high enough to capture all hydroxyl radicals generated in these conditions, since no O_2 production was observed in quenching runs.

Table 2
Elemental analysis of supports and iron-supported catalysts (%, w/w, d.b.).

Sample	C	H	N	S	O[a]	Ashes	Fe
CN	86.7	1	0.6	0.8	2.6	8.4	0.2
CNO	81.9	1.2	0.8	0.5	13.6	2	n.d.
1Fe/CN	85.9	1	0.7	0.6	3.7	8.1	1.1
4Fe/CN	78.1	1.2	0.8	0.7	7.6	11.6	4.2
4Fe/CNO	76.5	1.4	0.9	0.5	14.5	6.2	4.6
2Fe/CN	84.4	0.8	0.5	0.7	5.7	7.9	2.2
4sFe/CN	77.1	1.3	0.8	0.6	8.2	12	4.1
2sFe/CN	83.6	0.9	0.7	0.6	5.5	8.8	2.2

[a] By difference: %O = 100-(%C + %H + %N + %S + %Ashes).

Table 3
Porous structure of activated supports and iron-supported catalysts

Sample	S_{BET} ($m^2\ g^{-1}$)	A_{EXT} ($m^2\ g^{-1}$)	$V_{MICROPORE}$ ($cm^3\ g^{-1}$)	$V_{MESOPORE}$ ($cm^3\ g^{-1}$)	$V_{MACROPORE}$ ($cm^3\ g^{-1}$)	V_{TOTAL} ($cm^3\ g^{-1}$)
CN	1065	162	0.396	0.297	0.24	0.933
CNO	899	62	0.359	0.121	0.215	0.695
1Fe/CN	932	98	0.365	0.187	0.158	0.71
4Fe/CN	864	70	0.342	0.136	0.13	0.608
4Fe/CNO	965	84	0.383	0.16	0.141	0.684
2Fe/CN	915	91	0.357	0.177	0.142	0.676
4sFe/CN	895	78	0.349	0.151	0.138	0.638
2sFe/CN	834	75	0.327	0.145	0.138	0.61

3. Results and discussion

3.1. Physicochemical characterization studies

The commercial activated carbon is essentially constituted by C, with H, N and S in small proportions, as it can be seen in Table 2, which summarizes the elemental chemical analysis of CN supports and their corresponding iron-supported catalysts. The ashes content in the original activated carbon was essentially attributed to silica-alumina, traces of Mg, Ca and K, and a certain amount of Fe representing 0.2% by weight of AC [14]. Nevertheless, the ashes content in the treated CNO support was significantly lower than in the original CN at the same time that a higher oxygen percentage was also observed as a consequence of acidic treatment with HNO_3. Oxygen percentages of all the catalysts were always higher than those of the corresponding carbon supports, again due to the oxidizing character of iron nitrate solution used for the impregnation step and the final heat-treatment in air atmosphere. In all cases iron content of the catalysts accurately corresponds to the nominal iron content validating the iron-supported catalyst preparation method.

Table 3 shows the main parameters of the porous structure of activated carbon supports and iron-supported catalysts. All of them present very high surface areas, around 900 $m^2\ g^{-1}$, with type I adsorption isotherms corresponding to microporous materials. A significant contribution of meso and macroporosity (>43 %) was

Table 4
CO and CO2 evolved upon TPD and pHslurry.

Sample	CO (mmol g^{-1})	CO_2 (mmol g^{-1})	pH_{slurry}
CN	0.8	0.3	10.4
CNO	2.5	0.3	4.5
1Fe/CN	0.9	0.4	6.5
4Fe/CN	2.7	1.2	5.8
4Fe/CNO	3.7	1.3	3.2
2Fe/CN	1.9	0.5	6.1
4sFe/CN	2.6	1.1	5.1
2sFe/CN	1.8	0.6	5.4

Table 5
O/C and Fe/C atomic ratios of supports and iron-supported catalysts and mean diameter of iron particles of all iron-supported catalysts.

Sample	$(O/C)_{bulk}$	$(O/C)_{XPS}$	$(Fe/C)_{bulk}$	$(Fe/C)_{XPS}$	d_{Fe} (nm)
CN	0.02	0.046	0.0005	–	–
CNO	0.124	0.097	n.d.	–	–
1Fe/CN	0.032	0.095	0.003	0.009	–
4Fe/CN	0.073	0.159	0.012	0.025	5.5
4Fe/CNO	0.061	0.119	0.013	0.014	1.9
2Fe/CN	0.05	0.125	0.006	0.013	3.4
4sFe/CN	0.078	0.145	0.013	0.03	3.1
2sFe/CN	0.049	0.113	0.006	0.018	2.8

also appreciated in all cases. In general a decrease of surface area and pore volume was found in iron supported catalyst with respect to the original activated carbon support, most probably as a consequence of some pore blockage after iron deposition. It is known that the amount and nature of surface oxygen groups (SOGs) are by far the most important factors affecting the surface characteristics and final performance of catalysts based on activated carbon materials. Generally, as the quantitative analysis of the surface functional groups is not straightforward, different techniques, such as XPS or TPD-N_2 are used to assess the chemical nature of the SOGs in activated carbon-based catalysts. Therefore, to learn more about the chemical surface composition, some studies of TPD-N_2, XPS and pH_{slurry} measurements were carried out. In Table 4 pH_{slurry} values and the amount of CO and CO_2 evolved upon TPD-N_2 for all the studied supports and Fe/AC catalysts are given. Whereas pH_{slurry} value of CN support suggests an important basic character, an important decrease, fundamentally due to the acidic and oxidizing character of the iron nitrate used as precursor, was observed in all pH_{slurry} values of iron supported catalysts. The very low pH_{slurry} value observed for CNO support, indicative of the important acid surface character, was expected after having been previously submitted to nitric acid treatment. This parameter may be a good indicator of the SOGs nature and the electrical charge of the catalysts surface, since it can be assimilated to the pH at the point of zero charge (PZC) of the solid, when the surface electric charge exhibits a neutral net value [20]. The chemical nature of catalysts surface was performed by TPD analyses and the assessment of SOGs. According to literature criteria [21], CO_2-evolving groups mainly correspond to acidic SOGs or pyrone-like structures whereas CO-evolving groups have been associated to phenolic, carbonyl or anhydride groups. Thus, the evolution of most CO_2-evolving groups is associated to acidic surfaces whereas the evolution of higher amounts of CO can be related to neutral-basic surfaces. In a previous work, the CN support presented a complex distribution where the main contribution to CO_2-evolving groups was due to carboxylic, pyrone and lactone groups, joined to another two important contributions linked to phenol and carbonyl groups and a third weak peak assigned to anhydride groups [14].

Moreover, all iron-supported catalysts have shown a noticeably higher content of SOGs, as expected from the higher oxidizing power of iron nitrate. In agreement with the more acidic nature of their surfaces, CO_2-evolving groups should be more abundant, although additional CO may be formed to some extent by reaction of iron oxides with activated carbon support during TPD analyses [22]. The 4Fe/CNO catalyst prepared with the oxidized support, presented the higher amount of SOGs and the lowest pH_{slurry} value. However, no meaningful differences were found out in the amount of CO/CO_2 regardless of the impregnation steps, and only slightly pH_{slurry} variations were shown, more acidic for two-steps impregnated catalysts likely due to changes in the SOGs distribution.

XPS studies confirmed the higher concentration of SOGs in the catalysts as can be seen in Table 5 where O/C and Fe/C atomic ratios are given for carbon supports and their corresponding Fe/AC catalysts. In Fig. 1 it is shown, as an example, the spectra of C 1 s, O 1 s and Fe 2p corresponding to 4Fe/CN catalyst, taking into account that very similar XPS spectra were found in all cases. First, the C (1 s) spectrum has been deconvoluted in six symmetric peaks of Gaussian-Lorentzian type [23,24]. Besides the main peak at 284.5 eV corresponding to graphitic or aromatic carbon, another peak centered at 285.1 eV was associated with aliphatic carbon or structural defects [22,23]. Three more peaks, centered at 286.0, 287.0 and 288.5 eV, can be associated with C—O bonds of functional groups, such as phenol and/or ethers; with a C═O bond, as in the carbonyl group, and with —COOC-bond characteristic of carboxylic, anhydride, and/or ester groups. The last peak centered at higher energy, 290.5 eV, is associated with the interband peak, corresponding to $\prod \rightarrow \prod^*$ transitions.

In the case of O (1 s) XPS spectra five symmetric peaks have been deconvoluted. The first fitted peak at 530.0 eV can be associated to oxygen of the inorganic matter (O-In). The following four peaks, at 531.5, 532.9, 533.9 and 536.0 eV, have been assessed as C═O bonds characteristic of carbonyl and/or quinone groups; as C-O bonds characteristic of phenol, lactone, anhydride and/or ether groups; as (O═C—O—H) corresponding to carboxylic groups and to adsorbed water, respectively [20,25,26].

Table 6 shows the SOGs distribution according to XPS deconvolution of C 1 s and O 1 s spectral regions. No significant differences were observed in the C 1 s spectral region, thus, the analysis of the SOGs has been performed with the O 1 s results. As can be seen, the O-In contribution decreased after the acidic treatment as it could be expected due to the lower ashes content of CNO activated carbon. On the other hand, this contribution in the Fe/AC catalysts is also affected by the presence of iron. The contribution of carbonyl-quinone-like groups was significantly increased in the CNO support respect to the original CN activated carbon. The contribution of these groups was lower for the catalyst prepared with 2% of iron in two steps. Different results have been observed for C-O like structures where lower contributions were always found for catalysts than their corresponding supports. Thus, all the Fe/AC catalysts prepared with CN support, regardless of the single or two-steps impregnation procedure, showed the lowest contribution of this type of groups; whereas the highest contribution was observed in the case of 4Fe/CNO catalyst. Regarding carboxylic SOGs contribution, it was higher for the original CN support which was not heat-treated; these groups are labile and easily decomposed at higher than 200 °C temperatures. Finally, no significant differences were observed in the contribution of adsorbed H_2O among the catalysts, being the highest contribution for the bare CN. Concerning the XPS spectrum of the Fe 2p region (Fig. 1), the presence of a main band centered at 711.3 eV can be observed, accompanied by a secondary one 13.2 eV displaced to higher binding energy (724.5 eV), with an area ratio of 1:0.5, which corresponds to the characteristic values of Fe^{3+}, in addition to a satellite peak around 719.0 eV confirming the presence of Fe^{3+} species in the surface of all the studied catalysts, [27,28]. A comparison between surface and bulk

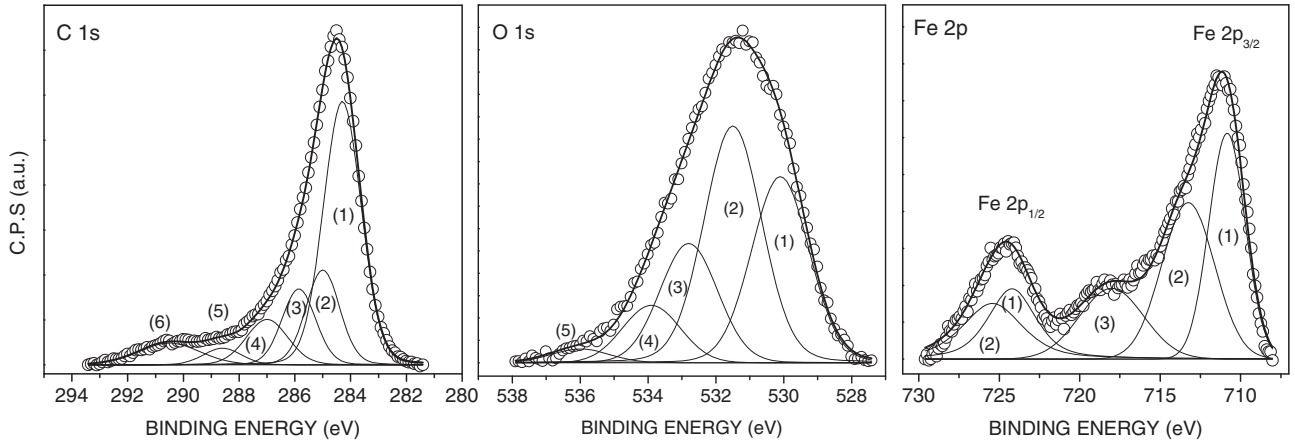

Fig. 1. XPS results of C 1 s, O 1 s and Fe 2p spectral regions of the 4Fe/CN catalyst.

Table 6
SOG distribution according to XPS deconvolution of C 1s and O 1s spectral regions.

Peak position (eV)	Assessment	% Contribution						
		CN	CNO	4Fe/CN	4Fe/CNO	2Fe/CN	4sFe/CN	2sFe/CN
C 1s								
284.4	C aromatic	44.5	42.5	42.2	45.3	46.8	43.1	45.6
285.1	C aliphatic	27.1	22.3	25.7	20.2	20.5	23.6	21.3
286	C—OH; C—O—C	11.4	14.8	11.9	12.4	13	10.5	12.4
287.1	C=O	6.5	10.2	9.4	8.9	6.5	9.6	5.9
288.5	COOH; COOC	3.6	3.4	4	6.5	5.9	6.2	6.1
290.5	Π→Π*	6.9	6.8	6.8	6.7	7.3	7	8.6
O 1s								
530	O—Fe; O—In[a]	12.2	4.5	30.3	20.7	29	30.1	30.9
531.5	C=O	33.9	43.3	39.3	35.1	39.3	36.2	35
532.9	C—O	31.8	38.5	19.2	32.9	18.7	20.3	18.7
534	COOH	16.9	10.2	9	7.6	9.8	11.3	11.7
536	H_2O_{ads}	5.1	3.5	2.2	3.7	3.2	2.1	3.7

[a] In: Inorganic impurities from the ash content in AC supports.

O/C atomic ratios can serve to describe the macroscopic distribution of SOGs in the catalyst particle (Table 5). Hence, in the case of CN support, since O/C_{XPS} is double than O/C_{bulk}, a higher density of oxygen groups is located in the most external surface [14], and could be reasonably concluded that these SOGs are distributed in the external AC surface, approaching to an egg-shell type configuration which could be beneficial to anchor iron active phases. On the contrary the treated support, CNO, presented lower density of SOGs by XPS, suggesting that they are more or less uniformly distributed in all (internal and external) AC surface. On the other hand, XPS analyses confirmed the higher concentration of oxygen groups in the surface of iron-supported catalysts as can be seen in Table 5. Although all of iron supported catalysts have always presented higher O/C_{XPS} ratios, those with lower iron content have even given rise to more than twofold of O/C_{XPS} values than their corresponding O/C_{bulk} ratios, which is pointing out very higher concentration of SOGs on their surfaces.

Finally, the comparison of Fe/C atomic ratios obtained by elemental and XPS analyses (Table 5) revealed that $(Fe/C)_{XPS}$ ratios were always higher suggesting that iron must be predominately located in the most external surface of the catalyst particles, except in 4Fe/CNO. This catalyst showed a uniform distribution of iron with similar XPS and bulk Fe/C ratios as a consequence of the concentration and distribution of SOGs in CNO support, which could favor the interaction of Fe-SOGs during preparation step. On the other side, catalysts prepared in two steps, 4sFe/CN and 2sFe/CN, presented $(Fe/C)_{XPS}$ ratios two or three fold than their corresponding $(Fe/C)_{bulk}$ values, that could well corroborate the location of iron species mainly in the most external surface of the catalyst particles, approaching to an egg-shell type distribution [12], and probably more accessible to reactants.

Comparative study of TEM micrographs (see Fig. 2) has shown significant differences. Calculated values of mean size of iron particles are also summarized in Table 5. Iron supported catalysts prepared by one-step incipient impregnation method (4Fe/CN and 2Fe/CN) have presented higher sizes of iron particles than the corresponding catalysts obtained in two-successive impregnation steps (4sFe/CN and 2sFe/CN), emphasized in the case of the highest Fe loading. Thus, two different mean sizes of iron particles, centered at 5.5 and 16.5 nm respectively, are pointing out the presence of important iron aggregates in 4Fe/CN catalyst surface, which was not observed in the case of 2% iron loading (2Fe/CN). On the contrary, a homogeneous distribution of iron particles, centered at c.a. 3 nm, was always observed in the case of iron supported catalysts prepared by two-steps impregnation method, regardless of the iron content. In the case of 4Fe/CNO, the very small size and homogeneous distribution of iron particles, around 1.9 ± 0.4 nm, should be underlined, what could be related to the SOGs concentration and distribution in the CNO support, favoring the interaction of iron with the activated carbon surface. In fact, the same phenomenon seems may be happening in the two-steps impregnation catalysts, where new SOGs were generated during the first impregnation-calcination step, avoiding iron agglomeration even with 4% of iron loading. Therefore, SOGs concentration and distribution are playing an important role in the distribution and size of iron particles in the surface of Fe/AC catalysts. In addition, both HNO_3 treatment of

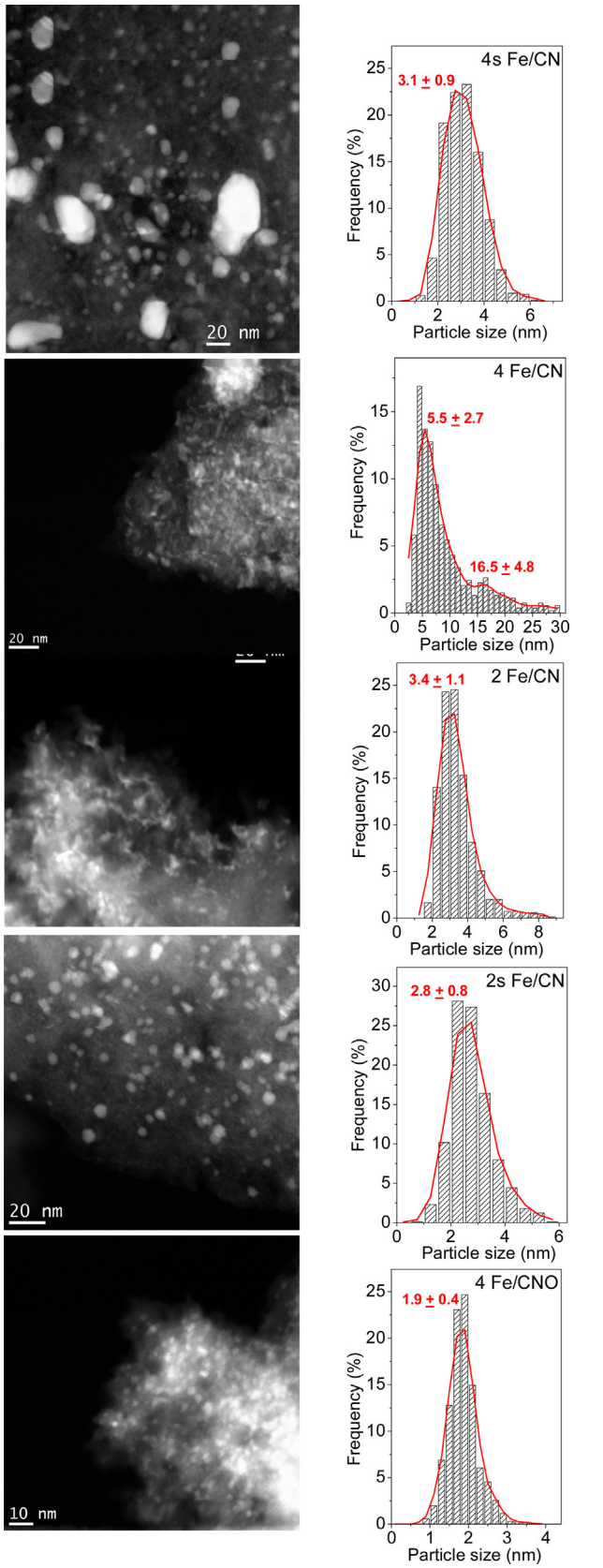

Fig. 2. HAADF-STEM images and particle size distribution of all iron-supported catalysts.

Table 7
TOC adsorption (initial and after CWPO treatment), TOC removal, mineralization percentage.

Catalyst	X_{ADS} Initial (%)	X_{TOC} (%)	X_{ADS} Final (%)	$X_{MINERALIZATED}$ (%)	$Fe_{LIXIVIATED}$ (%)
4Fe/CN	40	86.1	24.1	62	32
4Fe/CNO	34.6	77.7	21.4	56.3	34
2Fe/CN	46.5	88.3	25.3	63	31
4sFe/CN	40	86	23.2	62.8	26
2sFe/CN	44.6	86.5	25.1	61.4	25

the support or impregnation in successive steps can be an easy procedure to introduce iron species in Fe/AC catalysts at medium-high loading but preventing particles aggregation to some extent.

3.2. Catalytic activity

3.2.1. Batch experiments

Prior to phenol oxidation runs, phenol adsorption tests were carried out in order to discriminate adsorption from catalytic oxidation. The obtained results are given in Table 7 as adsorbed TOC (X_{ADS} initial, %) after 4 h of contact time. In a previous work, a high removal by phenol adsorption (around 1.1 mg phenol g^{-1} activated carbon, equivalent to 55% of phenol initial concentration) was observed for the original CN support [14], which was reduced to 46% for the CNO activated carbon. Regarding the catalysts, a decrease of 10–15% in the phenol removal by adsorption was found in all Fe/AC catalysts compared to the corresponding carbon supports. Taking into account that all the studied catalysts presented fairly similar textural properties, the differences found in their adsorption capacity should be mainly related to the variance in their surface properties more than as consequence of diffusional limitations. The most reduced phenol removal by adsorption corresponded to the 4Fe/CNO catalyst which presented the highest concentration of acidic SOGs and the lower pH_{slurry}, (see Table 4), in concordance with previous studies which conclude that phenol adsorption is diminished due to the presence of acid-type surface oxygen groups in the activated carbon surface [29–31].

The evolution of TOC and H_2O_2 concentrations during oxidation runs performed with all the studied catalysts is shown in Fig. 3, while Table 7 summarizes TOC conversions (X_{TOC}, %) after 240 min of reaction time. As observed, 4Fe/CN and specially 4Fe/CNO catalysts promoted a much faster decomposition of H_2O_2 in parallel to the poorest results in TOC removal, indicating a rather inefficient decomposition of hydrogen peroxide, that could be explained by two causes: (a) the high contribution of the H_2O_2 decomposition reaction towards O_2 non-reactive at the mild operating temperature of the experiments (50 °C) and/or (b) the very fast decomposition of H_2O_2 that provokes a high concentration of $^{\bullet}OH$ radicals in the initial stage which could favor auto-scavenging reactions. The poorest behavior was exhibited by 4Fe/CNO catalyst where the inefficient decomposition of H_2O_2 could be associated with the minimum and homogeneous sizes of iron particles characteristic of this catalyst that would not favor the oxidation process at the conditions studied here. On the other hand, catalysts with lower iron content or even those prepared by the two-steps impregnation method showed a significantly more efficient use of H_2O_2, with the H_2O_2 decomposition pathway probably taking place through the slow formation of $^{\bullet}OH$ radicals, being able to oxidize organic matter more easily due to their availability along the reaction. Thus, important TOC conversions were achieved after 60 min of reaction time with the less iron loaded catalysts, continuously increasing throughout the reaction while H_2O_2 was still decomposing. However, Fe/AC catalysts presented small differences attending to the

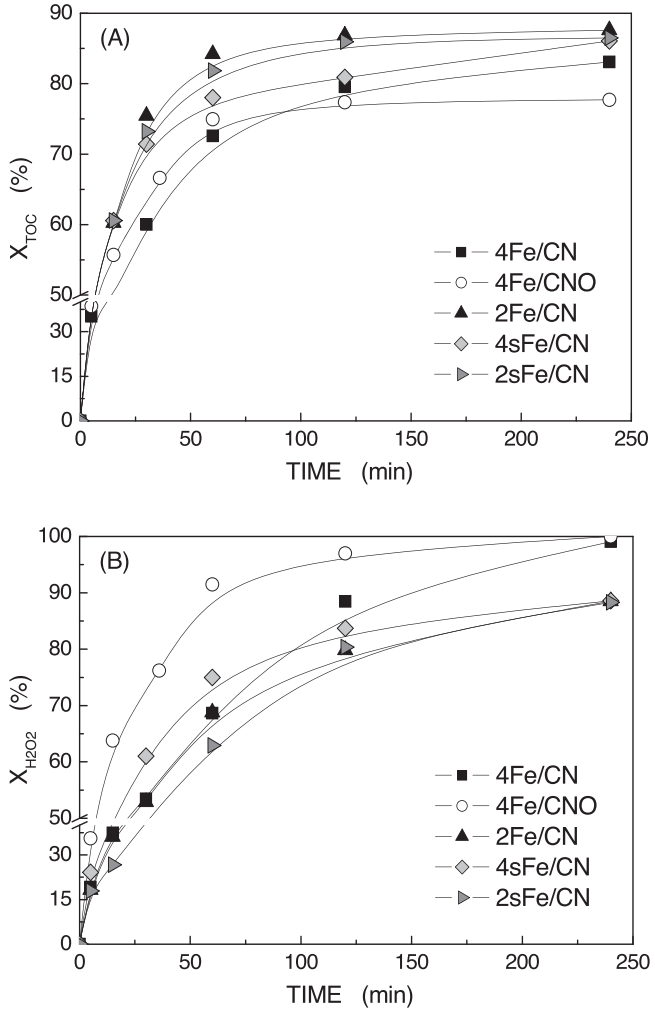

Fig. 3. Evolution of TOC (A) and H2O2 (B) conversions in CWPO of phenol with Fe/AC catalysts.

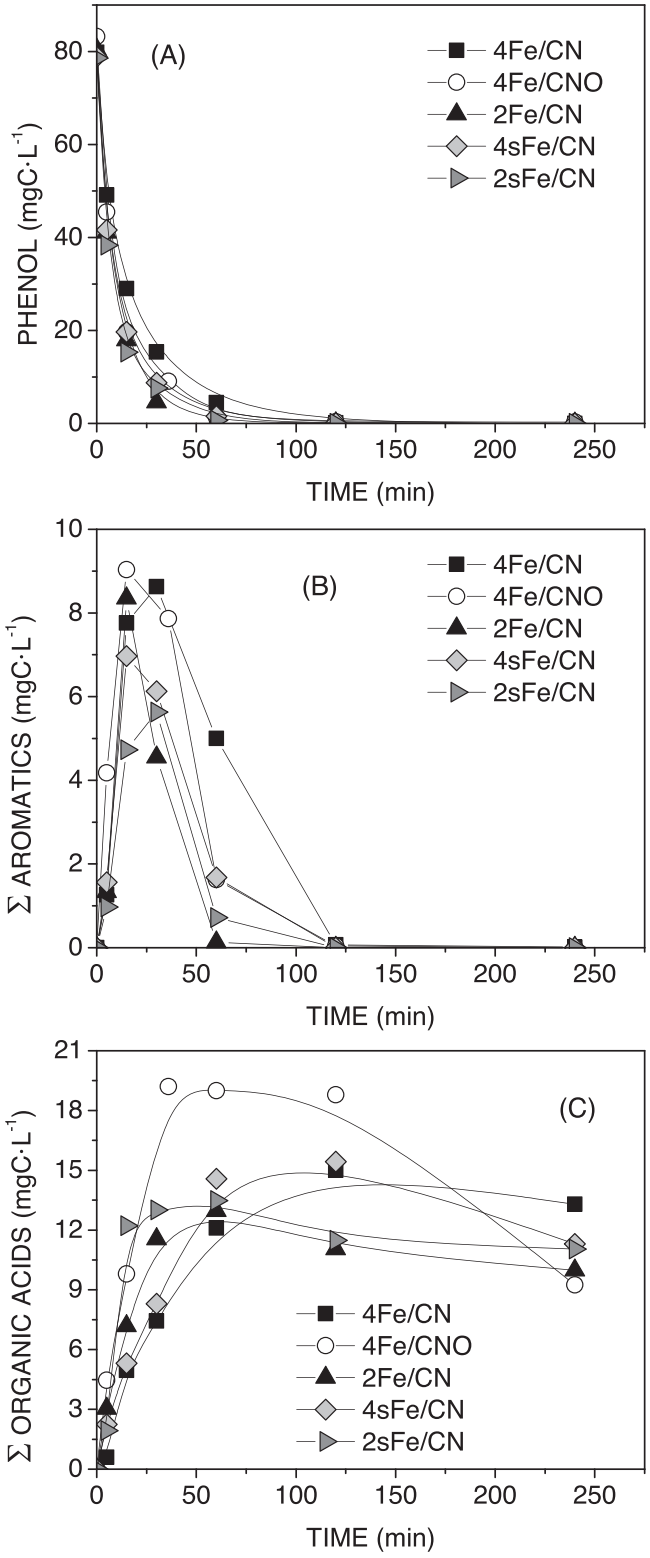

Fig. 4. Evolution of TOC corresponding to phenol (A), aromatic intermediates (B) and short-chain organic acids (C), in CWPO of phenol with Fe/AC catalysts.

iron loading, and only a slightly decrease in TOC removal was addressed with the increase of iron content.

It is known that phenol oxidation proceeds through a complex reaction scheme giving rise to some intermediate compounds before mineralization was reached, namely complete oxidation to CO_2 and H_2O [32,33]. Several intermediates, mainly aromatic and low weight organic acids have been always detected along this reaction. Catechol, p-benzoquinone and hydroquinone were always the primary oxidation intermediates as result of phenol hydroxylation, and they underwent further oxidation yielding organic acids, such as maleic, oxalic, formic and acetic, which were responsible of the final TOC detected in the reaction medium although without significance in terms of toxicity. The evolution of these intermediates and phenol were represented for all the studied catalysts in Fig. 4, in terms of equivalent carbon units (mgC L^{-1}). Aromatic and short-chain organic acids intermediates have been calculated as the sum of the corresponding compounds detected: catechol, p-benzoquinone and hydroquinone for aromatic compounds and maleic, oxalic, acetic and formic acids for short-chain organic acids.

Almost total phenol removal (99.9%) with the same concentration profiles along the operation time was achieved for all the studied catalysts after 60 minutes, in spite of some amounts of oxidation products still remain after 240 minutes of reaction time, as TOC conversions and the short chain organic acids concentration evolution, shown in Figs. 3 and 4 respectively, revealed. It is remarkably the highest short-chain organic acids concentration found between 30-120 minutes in the case of 4Fe/CNO catalyst.

Fe/AC catalysts may have at least two types of active sites in H_2O_2 decomposition reaction: AC sites, which could promote O_2 and/or •OH formation; and iron active sites which can generate H_2O_2 decomposition via •OH radicals. For this reason, different

Table 8
Yield of oxygen and •OH production in the presence of MeOH or Phenol during the catalytic hydrogen peroxide decomposition

Catalyst	Scavenger/Pollutant	Y_{O_2} (%)	Y_{OH} (%)
CN	MeOH	84.6	15.4
4Fe/CN	MeOH	64.4	35.6
4Fe/CNO	MeOH	69.8	30.2
2Fe/CN	MeOH	61.9	38.1
4sFe/CN	MeOH	64.1	35.9
2sFe/CN	MeOH	61.2	38.8
2sFe/CN	Phenol	43.2	56.8

runs were carried out to learn about the efficiency of H_2O_2 decomposition towards •OH generation. Quenching experiments with methanol (MeOH), a strong competitor for reactions •OH mediated in the liquid phase [13], could confirm the efficiency of •OH production and therefore, the true use of H_2O_2 consumption along CWPO reactions with Fe/AC catalysts. In the presence of high excess of MeOH, a known scavenger of •OH radicals (k=1 · 10^9 L mol^{-1} s^{-1}) [34], hydroxyl radicals will react mainly with it, decreasing the oxygen formed. Thus, the difference between oxygen formed with and without methanol, could be used as an indicator of the real •OH production during H_2O_2 decomposition in the presence of methanol. The inferior O_2 formation results obtained in all quenching runs confirmed the above postulated hypothesis [18].

Hydrogen peroxide decomposition rates in the presence of MeOH were slower than in the same MeOH-free experiment since methanol stops auto-scavenging reactions, such as those between •OH radicals and H_2O_2.

Considering the attained results for all the studied catalysts, reaction yields towards •OH and O_2 with MeOH, were calculated and summarized in Table 8. Higher hydroxyl radical production ($Y_{\bullet OH}$) during H_2O_2 decomposition reaction was achieved with the catalysts prepared with 2 wt.% of iron, being slightly increased in the case of two-steps impregnation catalyst. The minimum selectivity towards •OH radicals was observed for 4Fe/CNO catalyst that actually presented the maximum H_2O_2 decomposition rate. These results are according to the behavior observed during CWPO of phenol.

Therefore, quenching runs in the presence of a hydroxyl radical scavenger, as methanol, can be a useful tool to analyze the behavior of Fe/AC catalysts during CWPO processes. However, the selection of the target organic compound and the scavenger specie can play important roles in the overall process. Whereas methanol is not adsorbed onto the Fe/AC surface and some hydroxyl radicals could be being quenched by catalyst surface, an adsorbed organic molecule such as phenol over Fe/AC catalysts could block some centers of AC surface [35], responsible of the inefficient decomposition of H_2O_2. Finally, the presence of some cyclic aromatic compounds, such as hydroquinone/p-benzoquinone formed during this studied oxidation process, could even favor the reduction of Fe(III) species to Fe(II) on the catalyst surface, being Fe(II) the main responsible of hydroxyl radical generation [36–38].

Thus, going deeply into the effect of phenol instead of methanol along CWPO process over Fe/AC catalysts, the oxygen formed in the presence of phenol and the corresponding stoichiometric amount of H_2O_2, necessary to complete phenol oxidation, was evaluated with the catalyst that presented the highest hydroxyl production ($Y_{\bullet OH}$) during H_2O_2 decomposition, 2sFe/CN. Fig. 5 depicts the evolution of O_2 formed during the CWPO of phenol joined to the previous results for direct H_2O_2 decomposition and quenching runs with MeOH. A minor oxygen formation and slower hydrogen peroxide decomposition rate were obtained in the runs with phenol than in the presence of methanol, even when high excess of MeOH was use, which confirms the postulated beneficial effect that phenol adsorption could produce blocking some activated carbon sites where ineffective hydrogen peroxide decomposition takes preferably place towards H_2O and O_2.

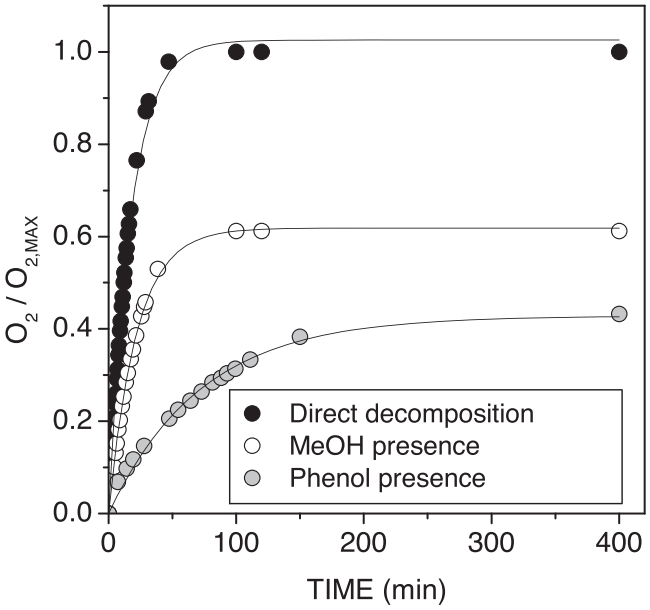

Fig. 5. Evolution of oxygen during direct hydrogen peroxide decomposition, and in the presence of methanol and phenol with the catalyst 2sFe/CN.

Both effects, the presence of aromatic intermediates as quinones, and the adsorption of phenol seem to increase the efficiency of H_2O_2 consumption during the CWPO of phenol, as suggested by the highest yield ($Y_{\bullet OH}$) given in Table 8, for the 2sFe/CN catalyst. This behavior could be extrapolated to the rest of the studied catalysts.

Attending to the role of adsorbed organic matter during and after CWPO reaction since TOC reduction could be also associated to adsorption in these catalysts tested in batch mode, the used catalysts after the CWPO of phenol were treated with NaOH to extract the adsorbed organic compounds onto the catalyst surface [15–17]. Previously, phenol adsorption on each catalyst was evaluated in dark conditions, and was expressed as X_{ADS} initial (%) in Table 7, as commented formerly. The amount of adsorbed TOC calculated by NaOH extraction compared to the initial TOC was expressed as X_{ADS} final (%) and represents the fraction of TOC that still remains adsorbed onto the catalyst surface after the treatment (Table 7). These obtained values have to be considered as semi-quantitative information, since the amount of phenol and aromatic intermediates extracted with NaOH in previous control runs with known amounts, was around 90% of the adsorbed quantity. Finally, the percentage of mineralization was calculated as following: $X_{MINERALIZED} = X_{TOC} - X_{ADS,final}$, also showed in Table 7. All the studied iron supported catalysts presented very similar percentages of adsorption (at the beginning or the end of the process) and final TOC conversion (X_{TOC} and $X_{MINERALIZED}$), and only the low adsorption, TOC and mineralization degree showed by 4Fe/CNO catalyst can be emphasized. Also it is remarkable the concordance of the mineralization reached with 2sFe/CN catalyst with the yield of hydroxyl radicals obtained in the presence of phenol.

Regarding to the catalysts stability, it is known that the presence of some refractory organic acids in the CWPO process, specially oxalic, can provoke an increase of iron lixiviates in the reaction medium as a consequence of the good stability of iron oxalates formed, which has already been reported as the main responsible of iron leaching from Fe-based catalysts [10,11,39]. For that, some experiments were carried out to investigate the stability of iron

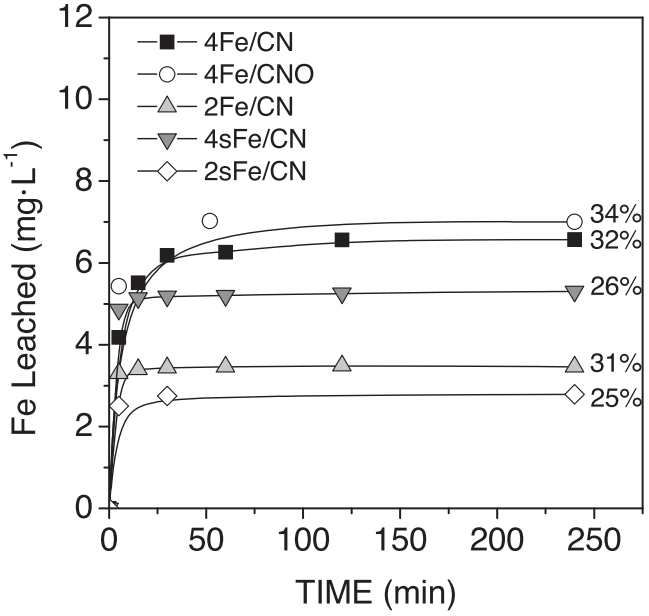

Fig. 6. Iron leached during stability tests with oxalic acid (25 mg L-1).

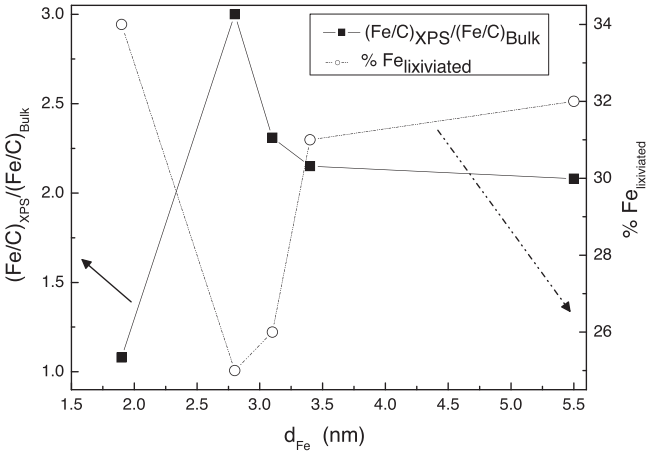

Fig. 7. Influence of iron particle size on catalysts stability (% Fe lixiviated) and surface iron content of the catalysts.

active phases on the catalysts in the presence of oxalic acid. These runs were performed in a batch reactor at the operating conditions described in the experimental section, using 25 mg L^{-1} oxalic acid solution which was superior to the maximum concentration found in the CWPO experiments after 4 h of reaction time. Although important iron lixiviates could be observed at the beginning of the CWPO process, the iron concentration was kept invariable after 60 min of reaction time (Fig. 6). However, from Figure 6 and summarized Table 7, some important differences can be emphasized when comparing all the catalysts. While higher iron lixiviates percentages were always addressed by the one step impregnation catalysts (4Fe/CN, 4Fe/CNO and 2Fe/CN), the best performance in terms of the oxalic acid stability test was observed for 2sFe/CN with the minor iron amount and prepared in two-consecutive steps.

In fact, all the catalysts prepared in one only step gave rise to around 31–34% of iron lixiviates, whereas those obtained by two-consecutive steps presented lower percentages. The improved stability could be pointing out to strengthened metal-support interaction, associated to the homogeneous iron particles with small sizes (≈3 nm) found in iron supported activated carbon catalysts prepared by two steps, 4sFe/CN and 2sFe/CN.

On the contrary, catalysts prepared by the one step impregnation method gave always rise to bigger iron particles with some particle aggregation as well. 4Fe/CNO catalyst, prepared from acid treated CN, presented the minimum iron particle size with the poorest stability in the reaction medium, maybe as a consequence of the lowest size and the highest dispersion of iron particles which could provoke a wider exposition of iron species to oxalic acid extraction or a poor metal–support interaction.

Under the reaction conditions, the possible contribution of homogeneous oxidation to phenol removal and mineralization with this type of iron supported catalysts can be considered negligible according to previous results [11,12].

The role of metal-support interactions and iron particles sizes on CWPO performance has been illustrated in Fig. 7, where the influence of mean diameter of iron particles (d_{Fe}), determined by TEM, on catalyst stability, expressed as percentage of iron lixiviates (% $Fe_{lixiviated}$), and the ratio of external and total iron content, defined as $(Fe/C)_{XPS}/(Fe/C)_{Bulk}$ relation has been represented. Fe/AC catalysts with the highest $(Fe/C)_{XPS}/(Fe/C)_{Bulk}$ ratios, which corresponded to catalysts prepared in two steps, showed the minor iron lixiviates. On the contrary, catalysts with the worst stability were the iron supported catalysts prepared by the one step conventional impregnation method in which large sizes of iron particles were detected. Finally, the lowest size of iron particles (1.9 nm) and $(Fe/C)_{XPS}/(Fe/C)_{Bulk}$ ratio were found in 4FeCNO catalyst which also presented the poorest stability of the series.

Concluding, Fe/AC catalysts prepared in two steps with 2 wt.% of final iron loading presented iron particles fundamentally located in the most external surface of the catalyst, approaching to an egg-shell type distribution with sizes of 3 nm that seems to lead to higher iron stability in the reaction medium as a consequence of the improved iron anchorage on activated carbon supports, what permits to achieve optimal results for the CWPO of phenol.

3.2.2. *Long-term experiment in continuous operation*

Finally to analyse the stability and durability of 2sFe/CN catalyst, a long-term experiment of CWPO of phenol was carried out in a CSTR for 180 hours of operation time. Fig. 8 summarizes iron lixiviates (A), evolution of TOC, phenol and H_2O_2 conversions (B), and the corresponding aromatic and short-chain organic acids by-products formed along CWPO reaction, Fig. 8 (C) and (D), respectively. It could be observed that the steady state was arisen after around 50 h, when the balance between adsorption breaking point and oxidation is reached and important iron lixiviation during the first 10 hours of operation is observed. After that, 2sFe/CN catalyst presented very good stability but moderate catalytic activity with 20% and 40% of TOC and phenol conversions, respectively. Phenol was not completely mineralized, and amounts of oxidation products remain after 180 h, that mainly correspond to p-benzoquinone, Fig. 8 (C), and short-chain organic acids, chiefly oxalic and acetic, Fig. 8 (D). Among the organic acids, oxalic deserves a particular attention because, as aforementioned, it is considered the primary responsible for the iron leaching in Fe-based catalysts [10,12], and it shows oxidation-resistance by the CWPO process investigated.

Main changes on the catalyst textural properties and iron content were analysed after the long-term experiment, together with the amount of organic compounds that still remained adsorbed onto the catalyst surface. These results are shown in Table 9 together with the corresponding values of the fresh catalyst for comparative purposes. It can be observed that iron loss in the catalyst was around 40%, quite similar to the value calculated from the lixiviation results, 35.4% (Fig. 8(A)). Besides, a significant decrease of textural parameters was observed after the oxidation treatment, higher than 50% in BET surface area and micropore volume. Since no very significant oxidation of the catalyst surface is expected at the mild conditions used in this work [19,20], these results are

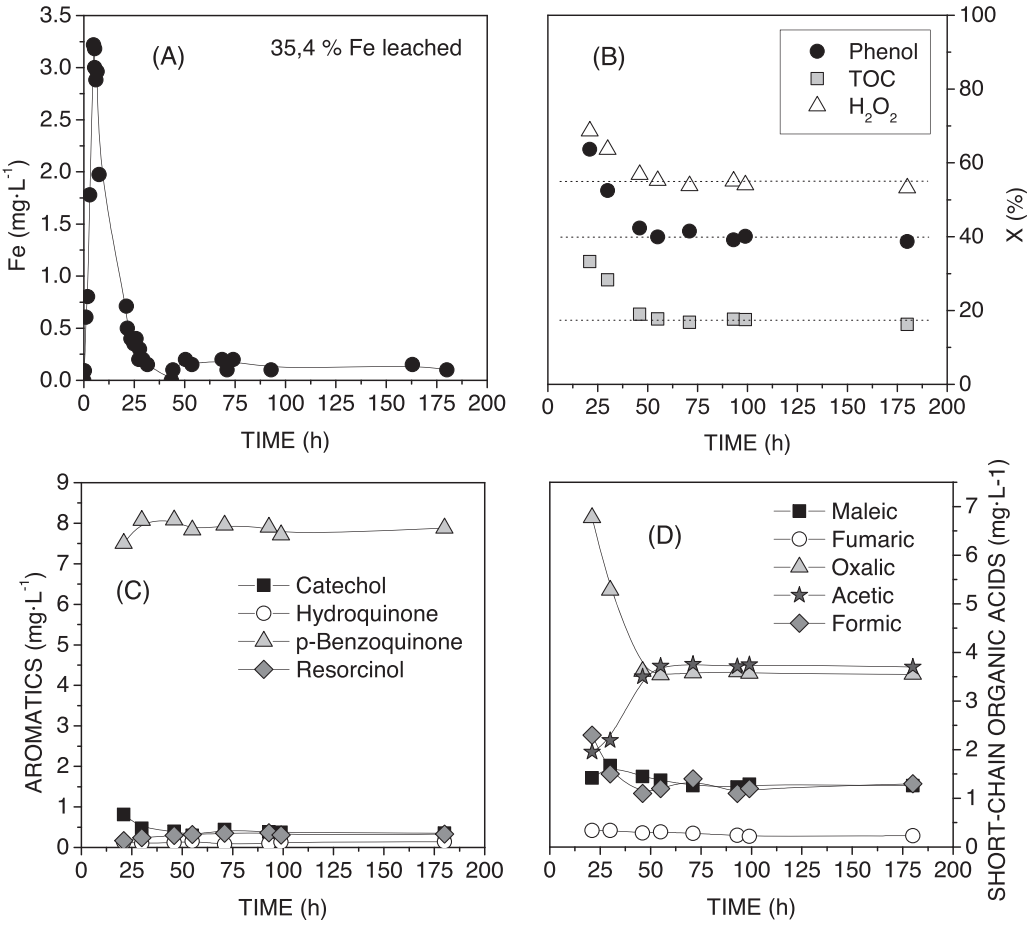

Fig. 8. Results of CWPO of phenol during long-term stability test with 2sFe/CN catalyst. Time evolution of (A) iron leached, (B) phenol, TOC and H2O2 conversions, (C) aromatic intermediates and (D) short-chain organic acids.

Table 9
Fresh and used 2sFe/CN catalyst characterization after long-term experiment.

Catalyst	Fresh 2sFe/CN	Used 2sFe/CN
Fe (%, w/w)	2.2	1.3
S_{BET} ($m^2\ g^{-1}$)	834	310
A_{EXT} ($m^2\ g^{-1}$)	75	100
$V_{MICROPORE}$ ($cm^3\ g^{-1}$)	0.327	0.099
V_{TOTAL} ($cm^3\ g^{-1}$)	0.61	0.349
Adsorbed TOC ($mg\ g^{-1}$)	0	51.2

compatible with the blockage of the microporous structure of the catalyst to some extent due to adsorbed organic compounds onto the catalyst surface. This has been previously reported for a similar Fe/AC catalyst in which washing with 1N NaOH aqueous solution led to the practically total recovery of its BET surface area, proving thus the role of the adsorbed organic matter in the blockage of the porous structure [11]. The extraction of the adsorbed organic matter after the treatment gave rise to a loading of around 50 mg TOC per g of the catalyst which sum around 17% of the TOC removed upon the treatment. Deeper and more extensive characterization to elucidate the nature of the adsorbed organic compounds is a need (condensed polymeric species, phenol or aromatic intermediates) and will be a part of future works together with thorough characterization of the iron active phase in the catalyst surface after the reaction.

Therefore, although two steps impregnation procedure significantly improves the Fe/AC catalysts stability for the CWPO of phenol, additional research efforts should be carried out to make them attractive for their use in continuous mode and boost their practical deployment.

4. Conclusions

A series of activated carbon-supported iron catalysts have been studied in the Catalytic Wet Peroxide Oxidation of phenol, analysing the influence of some variables: iron content, support oxidation and impregnation procedure, in their activity and stability during the process.

The oxidation of the support gave rise to a higher SOGs content in the catalyst and also the highest iron dispersion but both were in detriment of its catalytic activity and stability, leading a faster but inefficient decomposition of H_2O_2 during phenol oxidation and also a significant amount of iron leached. A decrease in the amount of iron from 4 to 2 wt.% led to lower SOGs content and increased iron dispersion when the catalysts were prepared in one step. However, the incorporation of iron in two impregnation steps provided exceptionally homogeneous distribution of iron particles, with sizes always centred at 3 nm, regardless of the iron content (2 or 4%). These catalysts presented improved stability, probably due to strengthened metal-support interactions as a consequence of the two steps of iron introduction each followed by calcination treatment. The best performance balanced between activity and stability was obtained during batch experiments with 2% iron 2-steps catalyst that gave rise to total removal of phenol after 60 min, and 86.5% TOC removal after 4 h.

Studies of H_2O_2 decomposition in the presence of an excess of $^{\cdot}OH$ scavenger as MeOH can be a useful tool to analyze the behavior

of heterogeneous catalysts along CWPO reactions. The selected catalyst, 2sFe/CN, led to better and efficient use of H_2O_2 with higher hydroxyl radical yield in the presence of phenol with respect to methanol, as a consequence of phenol adsorption over the catalyst surface that minimizes the inefficient decomposition of H_2O_2 towards oxygen, mainly catalyzed by AC active sites. Long-term experiment up to 180 h with this catalyst maintained a moderate-medium catalytic activity level with 40% phenol conversion and 20% TOC removal after the initial saturation of the catalyst and a 35% of iron loss during the 10 first hours.

Acknowledgements

This work has been supported by the Spanish Plan Nacional de I + D + i through the project CTM2010-14883/TECNO. A.B.H thanks the Ramon y Cajal program.

References

[1] M. Pera-Titus, V. García-Molina, M.A. Baños, J. Jiménez, S. Esplugas, Appl. Catal. B: Environ. 47 (2004) 219–256.
[2] Directive 2000/60/EC of the European Parliament and of the Council of 23 October 2000 establishing a framework for Community action in the field of water policy, Off. J. Eur. Communities, L327 (2000), pp. 1–72.
[3] S.T. Kolaczkowski, P.K. Plucinski, F.J. Beltrán, F.J. Rivas, D.B. McLurgh, Chem. Eng. J. 73 (1999) 143–160.
[4] Y.I. Matatov-Meytal, M. Sheintuch, Ind. Eng. Chem. Res. 37 (1998) 309–326.
[5] K. Pirkanniemi, M. Sillanpää, Chemosphere 48 (2002) 1047–1060.
[6] P.R. Gogate, A.B. Pandit, Adv. Environ. Res. 8 (2004) 501–551.
[7] F. Luck, Catal. Today 53 (1999) 81–91.
[8] F. Larachi, I. Illiuta, K. Belkacemi, Catal. Today 64 (2001) 309–320.
[9] W.H. Glaze, J.W. Kang, D.H. Chapin, Ozone Sci. Eng. 9 (1987) 335–352.
[10] S. Perathoner, G. Centi, Top. Catal. 33 (2005) 207–224.
[11] J.A. Zazo, J.A. Casas, A.F. Mohedano, J.J. Rodriguez, Appl. Catal. B: Environ. 65 (2006) 261–268.
[12] A. Rey, M. Faraldos, A. Bahamonde, J.A. Casas, J.A. Zazo, J.J. Rodríguez, Appl. Catal. B: Environ. 86 (2009) 69–77.
[13] A. Georgi, F.D. Kopinke, Appl. Catal. B Environ. 58 (2005) 9–18.
[14] A. Rey, M. Faraldos, A. Bahamonde, J.A. Casas, J.A. Zazo, J.J. Rodríguez, Ind. Eng. Chem. Res. 47 (2008) 8166–8174.
[15] A. Rey, J.A. Zazo, J.A. Casas, A. Bahamonde, J.J. Rodríguez, Appl. Catal. A: General 402 (2011) 146–155.
[16] C.C. Leng, N.G. Pinto, Ind. Eng. Chem. Res. 35 (1996) 2024–2031.
[17] N.H. Ince, I.G. Apikyan, Water Res. 34 (2000) 4169–4176.
[18] A. Rey, J. Carbajo, C. Adán, M. Faraldos, A. Bahamonde, J.A. Casas, J.J. Rodriguez, Chem. Eng. J. 174 (2011) 134–142.
[19] A. Rey, A. Bahamonde, J.A. Casas, J.J. Rodríguez, Water Sci. Technol. 61 (2010) 2769–2778.
[20] A. Moreno-Castilla, M.A. Ferro-García, J.P. Joly, I. Bautista-Toledo, F. Carrasco-Marin, J. Rivera-Utrilla, Langmuir 11 (1995) 4386–4392.
[21] J.L. Figueiredo, M.F.R. Pereira, M.M.A. Freitas, J.J.M. Orfao, Carbon 37 (1999) 1379–1389.
[22] J.A. Zazo, A.F. Fraile, A. Rey, A. Bahamonde, J.A. Casas, J.J. Rodríguez, Catal. Today 143 (2009) 341–346.
[23] H. Estrade-Szwarckopf, Carbon 42 (2004) 1713–1721.
[24] K. Ishimaru, T. Hata, P. Bronsveld, D. Meier, Y. Imamura, J. Mater. Sci. 42 (2007) 122–129.
[25] E. Desimoni, G.I. Casella, A. Morone, A.M. Salvi, Surf. Interface Anal. 15 (1990) 627–634.
[26] H. Darmstadt, C. Roy, S. Kaliagune, Carbon 32 (1994) 1399–1406.
[27] J.F. Moulder, W.F. Stickle, P.E. Sobol, K.D. Bomben, Handbook of X-Ray Photoelectron Spectroscopy: A Reference Book of Standard Spectra for Identification and Interpretation of XPS Data, Eden Prairie, Physical Electronics, USA 18,725, Lakedrive East, Chanhassen MN, 1995, pp. 55317.
[28] A.P. Grosvenor, B.A. Kobe, M.C. Biesinger, N.S. McIntyre, Surf. Interface Anal. 36 (2004) 1564–1574.
[29] C.H. Tessmer, R.D. Vidic, L.J. Uranowski, Environ. Sci. Technol. 31 (1997) 1872–1878.
[30] C.C. Leng, N.G. Pinto, Carbon 35 (1997) 1375–1385.
[31] M.W. Jung, K.H. Ahn, Y. Lee, K.P. Kim, J.S. Rhee, J.T. Park, K.J. Paeng, Microchem. J. 70 (2001) 123–131.
[32] R. Alnaizy, A. Akgerman, Adv. Environ. Res. 4 (2000) 233–244.
[33] A. Santos, P. Yustos, A. Quintanilla, S. Rodríguez, F. García-Ochoa, Appl. Catal. B Environ. 39 (2002) 97–113.
[34] G.V. Buxton, C.L. Greenstock, W.P. Helman, A.B. Ross, J. Phys. Chem. Ref. Data 17 (1998) 513–886.
[35] L.C.A. Oliveira, C.N. Silva, M.I. Yoshida, R.M. Lago, Carbon 42 (2004) 2279–2284.
[36] R. Chen, J.J. Pignatello, Environ. Sci. Technol. 3 (1997) 2399–2406.
[37] H. Gallard, J. De Laat, Chemosphere 42 (2001) 405–413.
[38] J.J. Pignatello, E. Oliveros, A. MacKay, Crit. Rev. Environ. Sci. Technol. 36 (2006) 1–84.
[39] F.J. Beltrán, F.J. Rivas, R. Montero-de-Espinosa, Water Res. 39 (2005) 3553–3564.